Acta Cryst. (1994). D**50**, 124–131

Structure Determination of Glucose Isomerase from *Streptomyces murinus* at 2.6 Å Resolution

BY HANNE RASMUSSEN

Department of Organic Chemistry, Royal Danish School of Pharmacy, Universitetsparken 2, DK-2100 Copenhagen, Denmark

TROELS LA COUR AND JENS NYBORG

Department of Chemistry, Aarhus University, Langelandsgade 140, DK-8000 Aarhus C, Denmark

AND MARTIN SCHÜLEIN

Novo Nordisk Industry A/S, Novo Allé, DK-2880 Bagsvaerd, Denmark

(*Received* 8 *October* 1992; *accepted* 10 *September* 1993)

Abstract

Glucose isomerase from *Streptomyces murinus* has been crystallized in space group $P4_12_12$, cell dimensions $a = b = 137.65$ and $c = 132.20$ Å. One dimer of the tetrametric molecule is found per asymmetric unit. An initial structure solution was obtained by the molecular replacement method. The crystallographic refinement was performed using molecular dynamics techniques with X-ray restraints. The final crystallographic R value is 21.4% at 2.6 Å resolution including 3023 non-H atoms, two metal ions and two water molecules per monomer.

Introduction

Xylose isomerase (E.C. 5.3.1.5), an enzyme present in a number of bacteria, catalyzes *in vivo* the isomerization of D-xylose to D-xylolose (Hochster & Watson, 1953). However, its ability to convert D-glucose to the sweeter D-fructose has given it great commercial interest, and xylose isomerase, XI is, therefore, often referred to as glucose isomerase, GI. Two divalent ions (Mg^{2+}, Mn^{2+}, Co^{2+}) per molecule are necessary to maintain biological activity (Kasumi, Hayashi & Tsumura, 1982).

A number of laboratories have studied the structure of GI isolated from different bacterial species by X-ray crystallography, with or without inhibitors or metal ions present, in order to understand and explain its mechanism of activity: XI, *Actinoplanes missouriensis*, 2.8 Å resolution (Rey *et al.*, 1988); XI, *Streptomyces olivochromogenes*, 3.0 Å resolution (Farber, Glasfeld, Tiraby, Ringe & Petsko, 1989); XI, *Arthrobacter*, 2.5 Å resolution (Henrick, Collyer & Blow, 1989); XI, *Streptomyces rubiginosis*, 1.9 Å resolution (Carrell *et al.*, 1989; Collyer, Henrick & Blow, 1990); XI, *Streptomyces albus*, 1.65 Å resolution (Dauter, Terry, Witzel & Wilson, 1990); XI, *Streptomyces rubiginosus*, 1.6 Å resolution (Whitlow *et al.*, 1991). The mechanism has been suggested to involve a metal-mediated 1,2 hydride shift (Collyer, Henrick & Blow, 1990, Whitlow *et al.*, 1991). Others have suggested a mechanism with an enediol intermediate such as that shown for triose phosphate isomerase (Rose, 1981; Carrell *et al.*, 1989).

GI is a tetramer, each monomer containing a domain folded as an eight-stranded α/β barrel, and a domain consisting of the C terminus, looping around the barrel of another molecule and thereby forming a tight dimer. This paper describes the structure determination of glucose isomerase from *Streptomyces murinus* to 2.6 Å resolution. The enzyme contains 388 amino acids per monomer giving a calculated molecular weight of 42 770 Da. GI from *Streptomyces murinus* shows a very large sequence identity with the isomerases from the *Streptomyces* species mentioned previously (more than 90%). The sequence identity compared to XI from *Arthrobacter* is 66%. One would, therefore, expect a large structural similarity, which is indeed the case. Structural differences are mainly observed on the surface and in the domain consisting of the C terminus.

The structure of GI from *Streptomyces murinus* has been determined in the presence of Mg^{2+}. Two metal positions are found. This will be discussed and compared to earlier results.

Experimental

Crystallization

Glucose isomerase from *Streptomyces murinus* was isolated and purified by Novo Nordisk A/S, Copenhagen, Denmark. Crystals were grown at room temperature by the sitting-drop vapor-

diffusion technique from 20 mg ml^{-1} GI solution in 0.4 *M* ammonium sulfate, 50 m*M* magnesium sulfate, TRIS buffer pH 8.5 against 2.0 *M* ammonium sulfate in TRIS buffer pH 8.5. The crystals are tetragonal bipyramids, which after repeated seeding reached a size of 1 mm and diffracted to about 2 Å resolution. From precession photographs the space group was determined to be $P4_12_12$ or its enantiomer $P4_32_12$ with cell parameters $a = b = 137.65$ and $c = 132.20$ Å. The asymmetric unit holds a dimer of molecular weight 85 540 Da ($V_m = 3.7$ Å^3 Da^{-1}). The tetramer is formed by crystallographic twofold symmetry.

Data collection

Because of slippage during data collection, crystals were mounted in glass capillaries between pipe-cleaner fibers and the crystal was coated with a film of polyvinylformal by allowing a solution of 2% polyvinylformal in 1,2-dichlorethane to evaporate from the capillary with the mounted crystal (Rayment, Johnson & Suck, 1977). Data were collected on an Arndt–Wonacott oscillation camera with three films per cassette. The X-ray source was a rotating Cu anode ($\lambda = 1.5412$ Å, 36 kV, 40 mA).

Oscillation angles between 0.2 and 0.3° were used, the crystal was rotated around the unique axis *c*. Two crystals were used to record 45° rotation at 2.6 Å resolution. The oscillation photographs were digitized by an Optronics film scanner with a 25 μm step size, and reduced and measured by the *MOSFLM* film-processing package (Leslie, Brick & Wonacott, 1986). Scaling and merging were performed using the *CCP*4 suite of programs supplied by SERC Daresbury Laboratory (1979). The statistical results of the data collection are shown in Table 1.

Table 1. *Summary of data collection*

a (Å)	137.65
b (Å)	137.65
c (Å)	132.20
Rotation angle (°)	0–41.4
No. of reflections with $I > 3\sigma$	31564
R_{merge} (%)	9.5
% of full data set at 2.6 Å resolution	85

Phase determination

A set of starting phases were obtained by molecular replacement techniques. The search model was a poly-alanine chain constructed from the C^α coordinates of xylose isomerase from *Arthrobacter*, kindly provided by Collyer, Henrick & Blow. The poly-alanine chain was constructed using the program *FRODO* (Jones, 1978). The search model was the tetramer generated from the dimer by symmetry operations. The tetramer was used as a search model after having tried both a monomer and a dimer without any success. The rotational and translational parameters were obtained using the *MERLOT* program package (Fitzgerald, 1988).

Using data between 10 and 6 Å resolution the highest peak found in the rotation-function map has an r.m.s. value 1.4 times higher than the second highest peak. The rotation-function map was generated from the results found by the Crowther fast-rotation function (Crowther, 1972). Using data between 8 and 5.3 Å resolution a clear, consistent solution for the translation function (Crowther & Blow, 1967) was revealed in the sections $x = \frac{1}{2}$, $y = \frac{1}{2}$ and $z = \frac{1}{2}$. In all three sections the highest peak was more than 1.5 times higher than the second highest one.

One clear solution to the rotation and translation function was thus obtained, placing the 222-symmetry center of the tetramer on a crystallographic twofold axis with one of the internal twofold axes identical to the crystallographic twofold axis [110], *i.e.* one dimer per asymmetric unit. Crystal packing considerations indicated that $P4_12_12$ was the correct space group since the solutions found for the rotation and translation functions in $P4_32_12$ would result in crystal packing with several overlapping molecules.

A $2F_o - F_c$ map was generated (*CCP*4 suite of programs) to 2.6 Å resolution, and an initial model of one of the monomers was built according to the sequence and density. At points where the density was unclear the model was built in such a way that optimal geometry was met. The model was built using the program *FRODO* and its refine routine for optimizing the geometry. This initial model contained coordinates for the full sequence, 388 residues (Luiten, Quax, Chuurhuizen & Mrabel, 1989). From this monomer the other monomer in the asymmetric unit was generated by a non-crystallographic symmetry operation.

Refinement

At the start, ten cycles of restrained least-squares refinement (LSQ1) using the program *PROLSQ* (Konnert & Hendrickson, 1980) were carried out. The *R* value dropped from 56.5 to 40.8% (10–3 Å resolution).

The model, together with the X-ray data, were subjected to molecular dynamics refinement with the *GROMOS* program package (van Gunsteren & Berendsen, 1987). The strategy used and the results are briefly outlined in Table 2. Initially energy minimization with X-ray restraints (EMX), using 10–3 Å resolution data lasting 0.3 ps (150 steps of 2 fs), was performed to further reduce the energy in the model.

Table 2. *Summary of the strategy and some of the results of restrained molecular dynamics (MD) refinement using the program package GROMOS*

EMX: energy minimization, X-ray restrained. MDX300: molecular dynamics, X-ray restrained, 300 K. MDX600: molecular dynamics, X-ray restrained, 600 K. Sig$F$: X-ray weight (the smaller sig$F$ the greater the weight at the X-ray term).

	Resolution (Å)	Sig$F$	No. of steps accumulated	R value (%)	CPU (h), MicroVAX 3100
EMX	10.0–5.0	500	100	37.7–38.9–38.4	9
EMX	10.0–3.0	500	150	45.3–41.0	9½
MDX300	10.0–5.0	750	250	38.4–39.7–33.3	12
MDX600	10.0–5.0	600	450	33.2–28.6	10
MDX600	10.0–5.0	400	550	28.5–21.6–21.4	16½
MDX600	8.0–4.0	600	650	38.7–30.7	10½
MDX600	8.0–4.0	400	750	30.5–24.2	10
MDX600	8.0–3.5	500	850	32.7–28.1	12½
MDX600	6.0–3.0	600	900	34.2–30.1	18
MDX600	6.0–2.6	500	1000	34.4–29.2	24½
MDX600	6.0–2.6	400	1050	29.1–27.4	11½
Manual rebuilding					
EMX	6.0–2.6	500	1150	28.5–26.0	16
EMX	6.0–2.6	400	1250	25.9–24.2	35
EMX	6.0–2.6	300	1310	24.2–22.9	13½

Refinement was performed according to the example given by Fujinaga, Gros & van Gunsteren (1989), except that the algorithm *SHAKE* was not used.

Several cycles of molecular dynamics refinement with X-ray restraints (MD) at 300 and 600 K were performed. In these cycles the resolution was gradually increased starting with low-resolution data (10–5 Å) and ending with all data between 6 and 2.6 Å resolution. The low-resolution data were omitted in the later cycles in order to avoid the solvent structure contribution. The weight of the X-ray term was varied as the refinement proceeded. These refinement cycles lasted 2 ps (1000 steps of 2 fs), and resulted in an R value of 27.0%.

At this point a small manual correction of the N- and C-termini of the two monomers took place using the program *FRODO*. Further cycles of EMX with a full data set (6–2.6 Å resolution) were performed lasting 0.6 ps (300 steps of 2 fs), decreasing the R value from 28.5 to 22.9%.

During the refinement the two monomers per asymmetric unit were regarded as two independent molecules, *i.e.* no non-crystallographic symmetry restraints were included in the refinement. The temperature factors were so far kept constant at 23.0 Å^2.

An electron-density map, $2F_o - F_c$, was generated. Using the molecular graphics program *O* (Jones, Zou, Cowan & Kjeldgaard, 1991) small corrections of some of the side chains and a few main-chain atoms were performed and two magnesium ions per monomer were included.

In order to optimize the geometry 80 cycles of least-squares refinement (LSQ2), using the program *PROLSQ* were performed including refinement of individual temperature factors. These cycles took place alternating with inspection of $2F_o - F_c$ and $F_o - F_c$ electron-density maps. The refinement converged at $R = 21.4\%$ for data between 6.0 and 2.6 Å resolution including 3023 non-H atoms, two metal ions and two water molecules per momomer. Because of the limited resolution of the data these two water molecules are the only two included in the structure.

Table 3. *R.m.s. deviations* (Å) *of* C^α *between the structure of GI at different points of the refinement (after superposition)*

MR: initial model (*Arthrobacter*) used for the molecular replacement. LSQ1: model after rebuilding and least-squares refinement using program *PROLSQ*. MD: model after molecular dynamics refinement. LSQ2: final model, after least-squares refinement using program *PROLSQ*.

	LSQ1	MD	LSQ2
Molecular replacement (MR)*	1.584	0.814	0.729
Least-squares refinement 1 (LSQ1)		0.935	0.894
Molecular dynamics refinement (MD)			0.528

* The number is the r.m.s. deviation between the generated tetramers from the dimer in one asymmetric unit, as the dimer present in the model MR (the open dimer) is different from the dimer (the tight dimer) in this structure.

Table 4. *Standard deviations after MD refinement and for the final coordinates*

	Standard deviation after MD	Standard deviation after LSQ2	No. of parameters
Distances (Å)			
Bond lengths	0.043	0.020	6178
Bond angles	0.120	0.046	8380
Dihedral angles	0.172	0.072	2174
Planar groups	0.103	0.028	
Non-bonded contacts (Å)			
Single torsion contacts	0.218	0.206	2197
Multiple torsion contacts	0.314	0.260	501
Torsion angles (°)			
Peptide plane	26.1	5.1	832
Staggered	29.3	26.4	1002
Orthonormal	36.6	36.0	98

Table 3 lists the r.m.s. deviations between C^α atoms after LSQ1, after MD and after LSQ2 compared to the molecular replacement solution and to one another. It is shown, that as the refinement proceeds the structural changes become smaller. The geometrical statistics after the molecular dynamics refinement and after the least-squares refinement are shown in Table 4. As the geometrical parameters after the MD refinement are not satisfactory, the final least-squares refinement (LSQ2) was performed. Fig. 1 shows the Ramachandran plot (Ramakrishnan & Ramachandran, 1965) of the refined coordinates of both molecules *A* and *B* in the asymmetric unit. Apart from glycines (marked with a cross) five residues have φ values greater than zero: Arg10, Glu186, Leu193, Asp257, Arg334 in both molecules *A* and *B*.

Glu186 precedes a *cis*-Pro and the remaining four residues have φ/ψ values not far from the allowed region for a left-handed α-helix.

The average temperature factor for all atoms is 20.3 Å^2. The individual average temperature factors for the main-chain atoms of molecules *A* and *B* are shown in Fig. 2. The temperature factors for the two metal ions are 12.0 and 17.1 Å^2 for site 1 and site 2 in molecule *A*, respectively, and 4.7 and 14.8 Å^2 for site 1 and site 2 in molecule *B*, respectively.

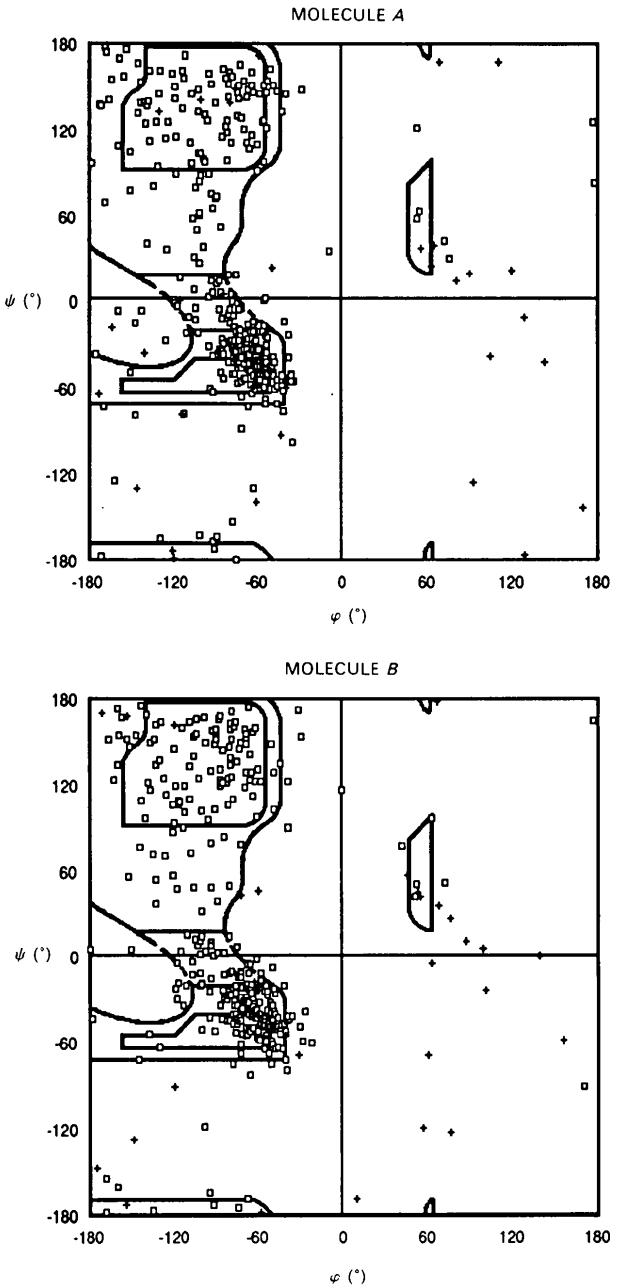

Fig. 1. Ramachandran plot for the final coordinates. Crosses (+) mark glycine residues, squares (□) other residues.

Results and discussion

The overall structure of this enzyme consists of two domains. One domain, at the N-terminus folds as an eight-stranded α/β-barrel and another domain, at the C-terminus makes an overall loop containing several α-helices. This overall loop folds around the barrel of another molecule thereby forming a dimer. Two such dimers compose the tetrametric structure. The N-terminal domain is made up of residues 1–322 and the C-terminal domain of residues 323–388. The secondary structure elements of the barrel are: β1 (Arg10–Gly14), α1 (Pro36–Lys46), β2 (Gly50–His54), α2 (Asp65–Ala81), β3 (Met84–Thr91), α3 (Arg109–Lys129), β4 (Thr133–Gly138), α4 (Val151–Gln172), β5 (Lys176–Pro184), α5 (Val196–Arg205), β6 (Val214–Glu217), α6 (Phe228–Ala238), β7 (His243–Lys246), α7 (Lys265–Ala278), β8 (Arg284–Asp287) and α8 (Phe296–Ala322).

Two metal ions are found in each monomer close to the C-terminal end of the β-strands and the following loops. Ligands to these ions are donated by β-strands 5, 6, 7 and 8 for metal ion 1, and from β-strand 6 and loops between β6 and α6, and β7 and α7 for metal ion 2. The C$^\alpha$ trace of molecule *A* and its two metal ions are shown in Fig. 3.

The barrel axes of the two subunits forming the dimer are almost perpendicular to one another, with the C-terminal domain packing along the side of the barrel of the other molecule close to the 20 amino-acid long helix, α3. The end of this helix almost sticks out through the C-terminal domain by four polar residues: Asn107, Asp108, Arg109 and Asp110.

The tetramer formed by crystallographic symmetry packs the two dimers in such a way that the

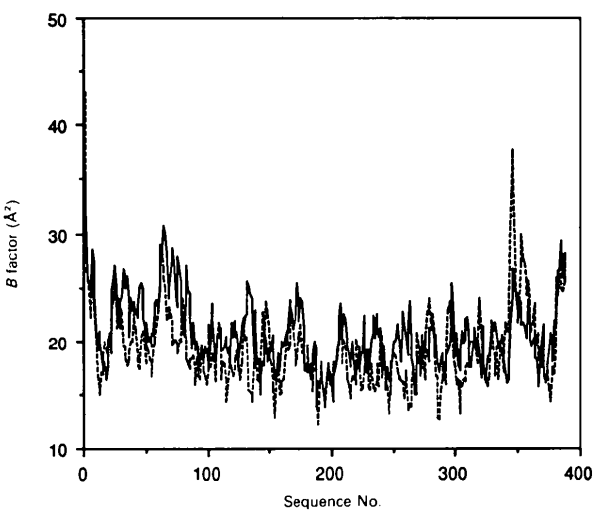

Fig. 2. The average temperature factor for the main-chain atoms of each residue for molecule *A* (solid line) and molecule *B* (dashed line) in the asymmetric unit.

C-terminal ends of the β-strands point against one another and thereby close the entrance into the barrel. The barrel axes of the crystallographically generated dimer are parallel to the axes of the original two barrels. In this way a hole is formed all the way through the two barrels from the N-terminus of one β-barrel to the N-terminus of another.

The access to the active site through the N-terminal end of the β-barrel is, however, almost totally blocked by a number of polar residues: Lys132, Thr133, Asp175, Arg177, Asn215 and His243. As a tetramer the only direct access to the active site is, therefore, *via* the site of the barrel, where an opening is formed between α1 and α2. As a dimer the active site, however, is easily reached from the C-terminus of the β-barrel.

In Fig. 4 the secondary structural elements are shown together with the differences between the structure of GI from *Streptomyces murinus* and that of XI from *Arthrobacter*, illustrated by the r.m.s. deviations between C^{α} atoms from the two structures. It can be seen that the largest differences are mainly observed in the C-terminus and in the loops between the β-strands and α-helices, but also large differences are found for α2; this, however, reflects a sequence identity for this helix of only 40%. Residues 343–353 are situated in the C-terminal domain in a region where only 35% sequence identity is observed over 20 residues.

As expected from the sequence homology, the overall structure compared with that of XI from *Arthrobacter*, as well as with structures of other published XI's, is very much conserved. This is also true for the active site, which in principle is identical to that observed in XI from *Arthrobacter*.

Ala343-Ala344-Asp345 is very poorly identified in the electron-density map in both molecules in the asymmetric unit. These amino acids are part of a loop between two helices in the domain forming the C-terminal 'arm' of one subunit. This is reflected in a large shift in coordinates during refinement and in the high temperature factor for these amino acids, especially for molecule *B* (Fig. 3). The electron density for Met1 is very weak.

It seems as if Ala262-Gly263-Asp264 can have two different positions in both molecules *A* and *B*. These amino acids are positioned in a loop between β7 and α7. During the molecular dynamics refinement these amino acids have actually been placed in two different conformations in the two molecules. An examination of the electron-density map after molecular dynamics refinement clearly showed two different 'routes' for Ala262-Gly263-Asp264, one being slightly more significant than the other in both molecules showing continuous density. The r.m.s. deviations of molecule *A* and molecule *B* after MD and after LSQ2 as a function of sequence number are shown in Fig. 5, and in Fig. 5(*a*) the differences in the positions of Ala262-Gly263-Asp264 are reflected. The elevated temperature factors (Fig. 3) for Gly263 of molecule *A* also show that this residue is not well determined. The r.m.s. deviations in C^{α} positions of Asp65 and Ser145 seem to be real according to the $2F_o - F_c$ electron-density map.

The two metal-binding sites per monomer were located in both the $2F_o - F_c$ (2.5σ) and difference

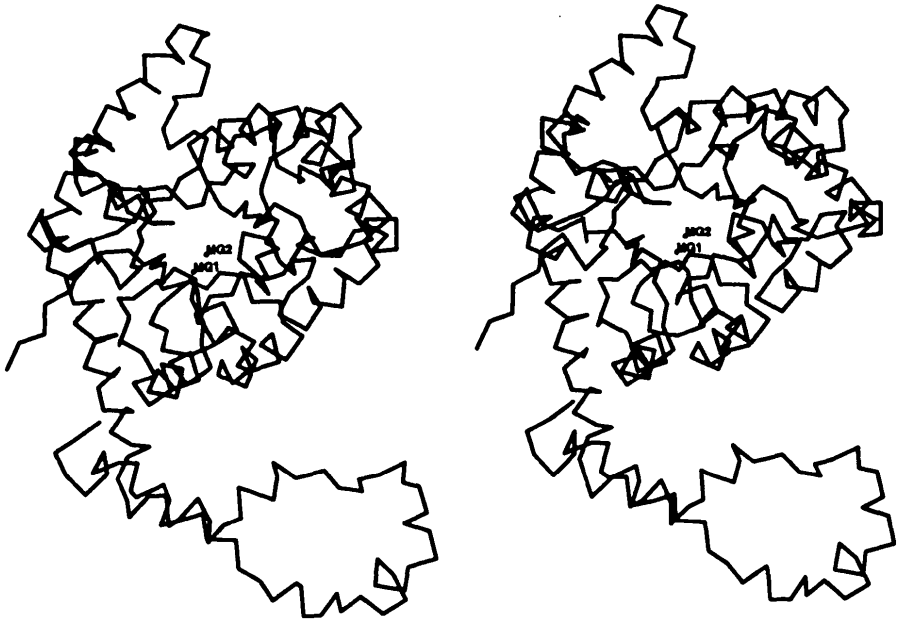

Fig. 3. Stereo drawing of the C^{α} of molecule *A* including the two Mg ions.

maps (3σ) in a late stage of the refinement after the molecular dynamics simulations. These positions are equivalent to those reported by a number of other groups (Dauter, Terry, Witzel & Wilson, 1990; Farber, Glasfeld, Tiraby, Ringe & Petsko, 1989; Collyer, Henrick & Blow, 1990; Carrell *et al.*, 1989; Whitlow *et al.*, 1991). However, several structures are reported as either metal free, or including both metal ions and an inhibitor or a substrate at the same time, and the presence of inhibitor or substrate seems to make a difference in the number of metal ions bound to the enzyme. The coordination of the two metal ions is shown in Table 5. Both ions are hexacoordinated, a sixth coordination to both metal site 1 and metal site 2 is to water molecules for which features are seen in $2F_o - F_c$ and $F_o - F_c$ electron-density maps. These two coordinating water molecules are the only two water molecules included in this structure determination. The structure of the metal site is shown in Fig. 6.

The two Mg^{2+} ions are placed with an interatomic distance of 5.0 and 4.7 Å in molecules *A* and *B*, respectively. This short distance between two metal ions is not often found in protein structures. In the October 1992 release of the Brookhaven Protein Data Bank (PDB, Bernstein *et al.*, 1977) only a few different structures are reported as having two divalent metal ions with an interatomic distance of less than 6.0 Å (leucine aminopeptidase, termolysin, concanavalin A, glutamine synthetase, parvalbumin and xylose isomerase). Furthermore, these structures are often determined in a complex with a ligand other than the metal ions.

Table 5. *Distances of coordination to the metal ions*

	Molecule *A* (Å)	Molecule *B* (Å)
Site 1		
Glu217 Oε1	2.1	1.8
His220 Nε2	2.8	3.0
Asp255 Oδ2	2.2	1.9
Asp255 Oδ1	2.6	2.6
Asp257 Oδ2	2.0	1.8
Water	1.8	1.8
Site 2		
Glu181 Oε1	2.6	2.7
Glu181 Oε2	2.1	2.3
Glu217 Oε2	2.1	2.1
Asp245 Oδ2	2.1	2.4
Asp287 Oδ2	2.3	2.4
Water	2.6	2.2

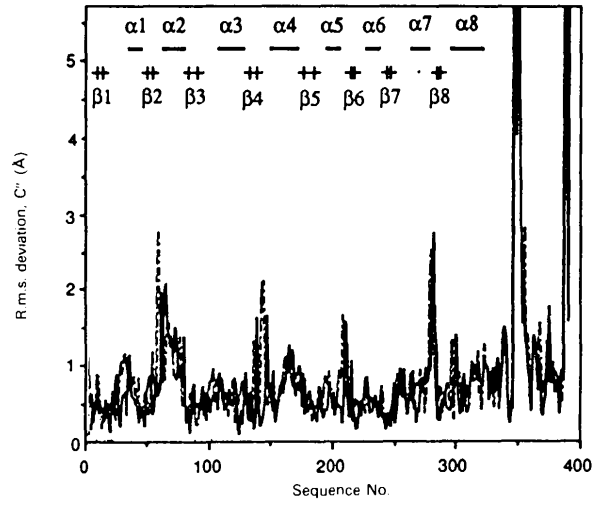

Fig. 4. R.m.s. deviations of C^{α} from *Streptomyces murinus* to XI from *Arthrobacter* for molecule *A* (solid line) and molecule *B* (dashed line). The secondary structure is illustrated at the top of the figure.

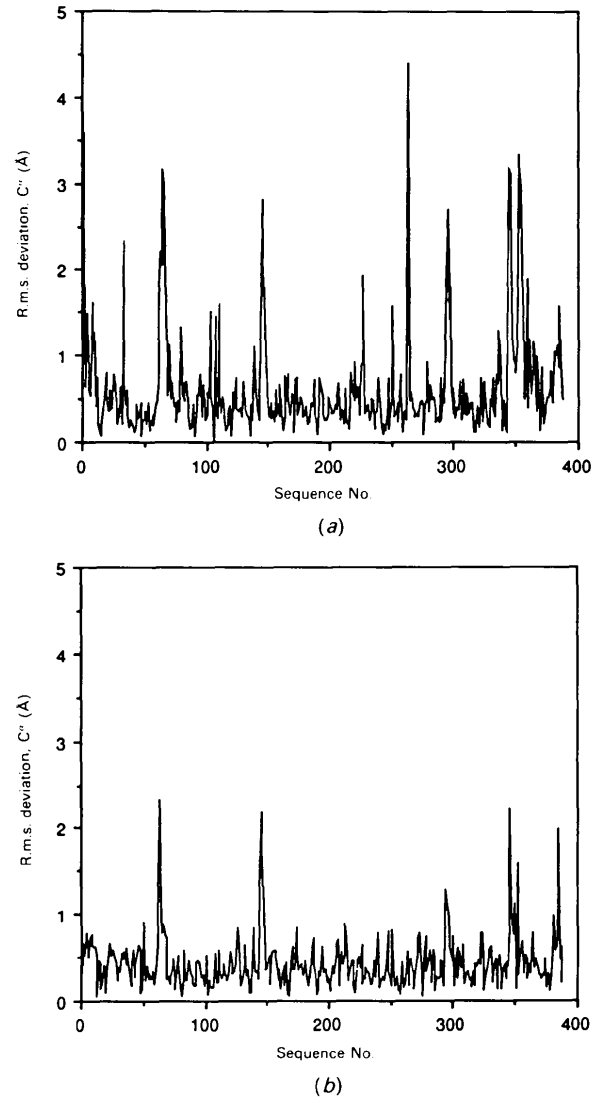

Fig. 5. R.m.s. deviations of C^{α} from molecule *A* to molecule *B* in the dimer of each residue (*a*) after molecular dynamics refinement and (*b*) for the final refined structure.

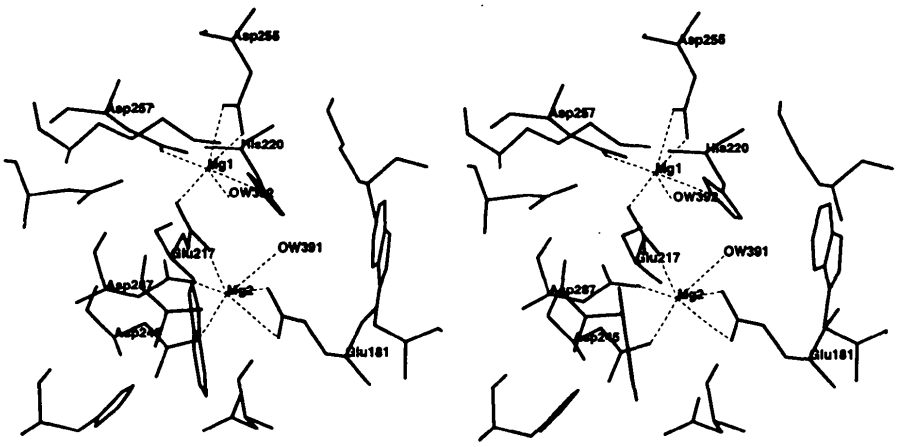

Fig. 6. Stereo drawing of the metal-binding site of molecule *A*.

One of the ligands for metal site 1 is His220. The coordination of histidine to a magnesium ion is not often recorded. In the release of the PDB previously mentioned only Rubisco has a histidine–magnesium coordination other than XI.

Collyer, Henrick & Blow (1990) have determined the structure of a number of XI derivatives of different metal ions with or without an inhibitor or a substrate. Among these, crystals soaked in 50 m*M* Mg^{2+} without inhibitor/substrate show that only one of the metal positions is occupied. The appearance of two magnesium ions per monomer in GI from *Streptomyces murinus* might be explained by the fact that they are cocrystallized in contrast to XI from *Arthrobacter* which was soaked with an equivalent concentration of Mg^{2+} at pH 8.0. Another explanation could be that the metal ion positioned in site 1 is not Mg^{2+} but Mn^{2+} left over from the isolation and purification of the enzyme, as suggested by Whitlow *et al.* (1991) after identification of two metal-binding sites in XI from *Streptomyces rubiginosis* which is cocrystallized in 0.5 m*M* Mg^{2+} at pH 7.0. A substitution of Mg^{2+} with Mn^{2+}, however, gives temperature factors at 33 and 27 $Å^2$ for metal site 1 for molecules *A* and *B*, respectively, values well above those expected. A final explanation might simply be that the difference observed for metal binding reflects a real difference between species. The structure of the coordinating amino acids of the metal-binding site in GI from *Streptomyces murinus* is otherwise quite similar to that reported for XI from *Arthrobacter* by Collyer, Henrick & Blow (1990).

number of mutations on XI from *Actinoplanes missouriensis* related to the metal-binding site of the enzyme. Among these the E186Q mutant is especially interesting in relation to the binding of Mg^{2+} *versus* Mn^{2+}. The mutant is inactive in the presence of Mg^{2+} but active with Mn^{2+}. van Tilbeurgh *et al.* found that the structure of the E186Q–Mg–xylose complex adopts another conformation of the metal-coordinating side chain of Asp255 compared to the wild-type complex and the E186Q–Mn–xylose complex. In the former Asp255 interacts with Gln186 instead of the Mg^{2+} in site 1 giving a less strong binding of this ion. This is not the case in the Mn complex. Therefore, it seems as if Mn^{2+} has a stronger affinity than Mg^{2+} for site 1, which might explain why metal site 1 is not always occupied by Mg^{2+} when a substrate/inhibitor is not present.

The coordinates have been deposited in the Brookhaven Protein Data Bank.*

K. Henrick, C. A. Collyer and D. M. Blow are thanked for kindly providing the coordinates of xylose isomerase from *Arthrobacter*. Colleagues at the University of Aarhus and at the Royal Danish School of Pharmacy are thanked for fruitful help during this work. The Danish Academy of Technical Sciences and Pharmabiotec are acknowledged for financial support.

* Atomic coordinates and structure factors have been deposited with the Protein Data Bank, Brookhaven National Laboratory. Free copies may be obtained through The Technical Editor, International Union of Crystallography, 5 Abbey Square, Chester CH1 2HU, England (Supplementary Publication No. SUP 37104). A list of deposited data is given at the end of this issue.

References

Bernstein, F. C., Koetzle, T. F., Williams, G. J. B., Meyer, E. F. Jr, Brice, M. D., Rodgers, J. R., Kennard, O., Shimanouchi, T. & Tasumi, M. (1977). *J. Mol. Biol.* **112**, 535–542.

Carrell, H. L., Glusker, J. P., Burger, V., Manfree, F., Tritsch, D. & Biellmann, J.-F. (1989). *Proc. Natl Acad. Sci. USA*, **86**, 4440–4444.

Collyer, C. A., Henrick, K. & Blow, D. M. (1990). *J. Mol. Biol.* **212**, 211–235.

CROWTHER, R. A. (1972). *The Molecular Replacement Method*, edited by M. G. ROSSMANN, pp. 173–178. New York: Gordon & Breach.

CROWTHER, R. A. & BLOW, D. M. (1967). *Acta Cryst.* **23**, 544–548.

DAUTER, Z., TERRY, H., WITZEL, H. & WILSON, K. (1990). *Acta Cryst.* B**46**, 833–841.

FARBER, G. K., GLASFELD, A., TIRABY, G., RINGE, D. & PETSKO, G. A. (1989). *Biochemistry*, **28**, 7289–7297.

FITZGERALD, P. M. D. (1988). *J. Appl. Cryst.* **21**, 273–278.

FUJINAGA, M., GROS, P. & VAN GUNSTEREN, W. F. (1989). *J. Appl. Cryst.* **22**, 1–8.

GUNSTEREN, W. F. VAN & BERENDSEN, H. J. C. (1987). *BIOMOS. Biomolecular Software*. Laboratory of Physical Chemistry, Univ. of Groningen, The Netherlands.

HENRICK, K., COLLYER, C. A. & BLOW, D. M. (1989). *J. Mol. Biol.* **208**, 129–157.

HOCHSTER, R. M. & WATSON, R. M. (1953). *J. Am. Chem. Soc.* **75**, 3284–3285.

JONES, T. A. (1978). *J. Appl. Cryst.* **11**, 268–272.

JONES, T. A., ZOU, J.-Y., COWAN, S. W. & KJELDGAARD, M. (1991). *Acta Cryst.* A**47**, 110–119.

KASUMI, T., HAYASHI, K. & TSUMURA, N. (1982). *Agric. Biol. Chem.* **46**, 21–30.

KONNERT, J. H. & HENDRICKSON, W. A. (1980). *Acta Cryst.* A**36**, 344–350.

LESLIE, A. G. W., BRICK, P. & WONACOTT, A. J. (1986). *CCP4 News*, **18**, 32–39.

LUITEN, R. G. M., QUAX, W. J., CHUURHUIZEN, P. W. & MRABEL, N. (1989). European Patent Application 8 921 892.0.

RAMAKRISHNAN, C. & RAMACHANDRAN, G. N. (1965). *Biophys. J.* **5**, 909–933.

RAYMENT, I., JOHNSON, J. E. & SUCK, D. (1977). *J. Appl. Cryst.* **10**, 365.

REY, F., JENKINS, J., JANIN, J., LASTERS, I., ALARD, P., CLAESSENS, M., MATTHYSSENS, G. & WODAK, S. (1988). *Proteins Struct. Func. Genet.* **4**, 165–172.

ROSE, I. A. (1981). *Philos. Trans. R. Soc. London Ser. B*, **293**, 131.

SERC Daresbury Laboratory (1979). *CCP4. A Suite of Programs for Protein Crystallography*. SERC Daresbury Laboratory, Warrington WA4 4AD, England.

TILBEURGH, H. VAN, JENKINS, J., CHIADMI, M., JANIN, J., WODAK, S. J., MRABET, N. T. & LAMBEIR, A.-M. (1992). *Biochemistry*, **31**, 5467–5471.

WHITLOW, M., HOWARD, A. J., FINZEL, B. C., POULOS, T. L., WINBORNE, E. & GILLILAND, G. L. (1991). *Proteins Struct. Funct. Genet.* **9**, 153–173.